

Femtosecond coherent transient infrared spectroscopy of CO on Cu(111)

J. C. Owrutsky

*Laboratory for Research on the Structure of Matter and Department of Chemistry,
University of Pennsylvania, Philadelphia, Pennsylvania 19104*

J. P. Culver

*Laboratory for Research on the Structure of Matter and Department of Physics,
University of Pennsylvania, Philadelphia, Pennsylvania 19104*

M. Li, Y. R. Kim, and M. J. Sarisky

*Laboratory for Research on the Structure of Matter and Department of Chemistry,
University of Pennsylvania, Philadelphia, Pennsylvania 19104*

M. S. Yeganeh and A. G. Yodh

*Laboratory for Research on the Structure of Matter and Department of Physics,
University of Pennsylvania, Philadelphia, Pennsylvania 19104*

R. M. Hochstrasser

*Laboratory for Research on the Structure of Matter and Department of Chemistry,
University of Pennsylvania, Philadelphia, Pennsylvania 19104*

(Received 20 April 1992; accepted 1 June 1992)

Femtosecond infrared coherent transients have been measured for the stretch vibration of CO on Cu(111). The free induction decay exhibits a dephasing time (T_2) of 2 ± 0.3 ps (and 2 ± 0.1 ps assuming a single exponential decay between 2 and 3 ps). The decay was best fit by exponential relaxation, thereby suggesting that the CO vibrational band is almost entirely homogeneously broadened. The surface sum frequency spectrum was also measured at two coverages (0.10 and 0.45 L) using spectrally narrowed pulses. Interferences were observed leading to a determination of the relative phase and amplitude of the resonant and nonresonant second-order susceptibility in this system. The magnitude of the nonresonant susceptibility was only weakly dependent on coverage, suggesting that the nonresonant polarizability originates in the bulk Cu. Time and frequency domain results were in good agreement.

I. INTRODUCTION

Measurements of vibrational energy and coherence relaxation are essential for a comprehensive description of surface adsorbate systems. Vibrational relaxation rates are often extracted from vibrational spectra,¹ but direct time-resolved measurements generally provide information free from assumptions about the dynamics. Recent experiments combining ultrafast infrared (IR) spectroscopy with ultra-high vacuum (UHV) techniques have reported vibrational energy relaxation rates for adsorbates on metal surfaces.² For example, IR pump-probe schemes were employed to measure vibrational energy relaxation times (T_1) of Cd stearate/Ag (Ref. 3), CH₃S/Ag(111) (Ref. 4), CO/Pt(111) (Ref. 5), and CO/Cu(100).⁶

A thorough characterization of the vibrational dynamics requires measurement of both population and coherence relaxation rates. Population relaxation times have been measured for vibrations of adsorbates on metals, but no experiments aimed at probing coherences have been carried out thus far. On the other hand, free induction decay (FID) and photon echo experiments to probe coherence in a semiconductor-adsorbate [H/Si(111)] system have been reported.⁷ In this case the relaxation rates were relatively slow (> 10 ps),⁸ so that transients were resolved with 7 ps pulses. Coherent transient measurements of adsorbates on metal surfaces however, require better time resolution because electron-hole pair-induced damping

mechanisms are about an order of magnitude faster than on nonmetals.

In this paper we report the first measurement of a vibrational coherent transient for an adsorbate on a metal surface. We have determined the vibrational dephasing rate (T_2) for CO on Cu(111) by obtaining the free induction decay signal. A short IR pulse (380 fs) generates the vibrational coherence and its temporal evolution is measured by upconverting the decaying surface polarization with a delayed visible pulse. Few IR experiments have been reported with comparable time resolution,⁹ and ours is the fastest for a surface IR experiment to date.

We have chosen CO on Cu(111) because its adsorption properties and steady-state vibrational parameters have been well characterized.^{10,11} In addition, time-resolved adsorbate studies have been performed on this and similar systems. For example, the laser-induced desorption time for CO on Cu(111) has been measured to be < 325 fs,¹² and the vibrational population relaxation time was measured to be ~ 2 ps for CO on Cu(100).⁶ The latter work used the same adsorbate and substrate as in the present experiments, but the surface plane is different. Studies of these systems present a unique opportunity to assess the effects of geometry and electronic structure on the adsorbate vibrational dynamics. Differences in IR linewidths have already been observed as a function of temperature for CO on Cu(111), but the linewidth for CO on Cu(100) is temperature independent.¹⁰

The coherent transient measurements reported here represent progress toward IR photon echo spectroscopy for adsorbates on metal surfaces. This capability will permit measurement of both population and pure dephasing relaxation rates for adsorbate vibrations. The present work also demonstrates the importance of pulse shape in the analysis of coherent transients to obtain correct relaxation times.

In addition to the FID measurement, we have measured the frequency domain surface sum frequency generation (SFG) spectrum for CO on Cu(111) using spectrally narrowed IR pulses at two coverages, 0.10 and 0.45 L. The spectra, especially at low coverage, display an interference which was analyzed to determine the relative amplitude and phase of the resonant and nonresonant parts of the second-order susceptibility. The total dephasing time and linewidth obtained in the time and frequency domains, respectively, are self-consistent. The values also agree with those reported previously in surface Fourier-transform infrared (FTIR) studies.¹⁰

II. EXPERIMENTAL

In the free induction decay measurement, we coherently excite CO adsorbed on Cu(111) with a 380 fs IR pulse and interrogate the temporal evolution of the coherence by measuring the variation of a surface-induced up-conversion signal with a 280 fs visible pulse that is delayed with respect to the IR pulse. Spectrally narrowed IR pulses (2 cm^{-1} , 10 ps) were used to obtain the surface SFG spectra as a function of IR frequency at two coverages. In both cases gated photon counting was employed to detect the SFG signal.

Our apparatus involves integration of an ultrafast IR laser system with an ultrahigh vacuum system as shown in Fig. 1. The sample was housed in an UHV chamber with a base pressure of 1×10^{-10} Torr. The chamber is equipped with standard surface cleaning and diagnostic instrumentation, including an ion gun, mass spectrometer, low energy electron diffraction (LEED), and double pass cylindrical mirror analyzer for Auger spectroscopy. The chamber was outfitted with CaF_2 windows to transmit the IR. The sample was a 1.8 cm diameter, 2 mm thick copper crystal cut at 2.5° with respect to the (111) crystallographic plane. Alternate cycles of Ar^+ sputtering for 20 min at 0.5 kV followed by flash annealing to 450°C were used to clean the sample. Auger spectra reveal $< 1\%$ impurities (carbon and sulfur) after cleaning. Weekly cleaning by sputtering and annealing as well as daily flash annealing were used to maintain the surface purity. Experiments were performed at 93 K by bringing the crystal into thermal contact with a liquid nitrogen cooled reservoir.

The adsorption properties of CO on Cu(111) have been previously reported¹⁰ and the overlayer structure was confirmed for our system using LEED. CO adsorbs molecularly through the carbon atom on atop sites for exposures < 0.45 L at 95 K. Experiments were performed on an ordered overlayer, $(\sqrt{3} \times \sqrt{3})R30^\circ$, corresponding to $\frac{1}{3}$ monolayer. This was obtained following an exposure of 0.45 L of

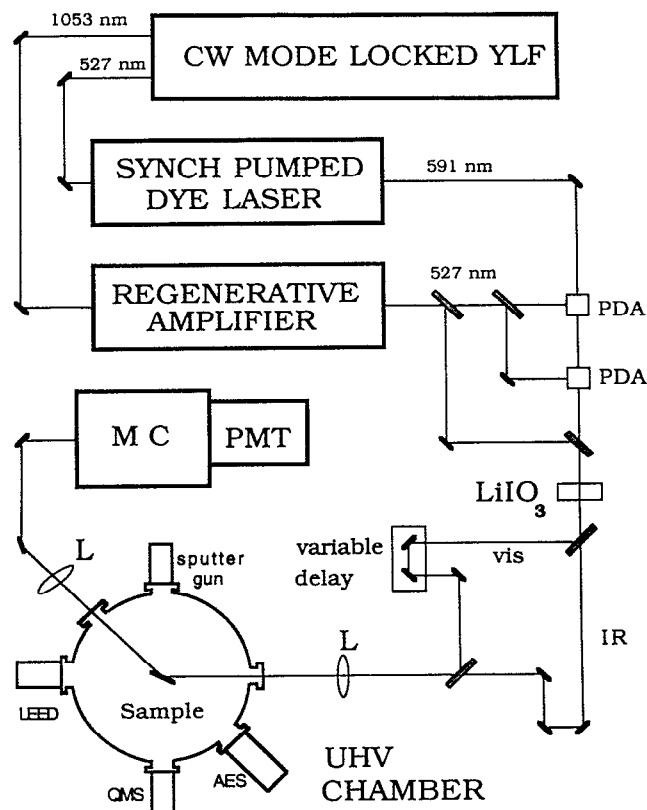


FIG. 1. Schematic of the apparatus used to measure the free induction decay and surface sum frequency spectrum for CO on Cu(111). PDA, pulsed dye amplifier cells; L, lenses; MC, a monochromator; PMT, photomultiplier tube; AES, Auger electron spectrometer; LEED, low energy electron diffraction; QMS, quadrupole mass spectrometer.

CO at 93 K. The CO was introduced into the chamber through a liquid nitrogen trapped reservoir. We confirmed the intended overlayer structure by observing the previously reported hexagonal LEED pattern¹⁰ in our system. The coverage was routinely monitored using second-harmonic generation (SHG) as described below.

The laser system uses a cw mode-locked Nd:YLF laser as the master oscillator. The frequency doubled output synchronously pumps a linear, dual-jet dye laser and the remaining fundamental seeds a regenerative amplifier. The frequency doubled output of the regenerative amplifier (1 mJ at 527 nm, 1 kHz, 60 ps) was used to amplify the dye pulses and generate IR. The dye laser employed in these experiments is based on a previously reported design.¹³ Briefly, it is a hybrid mode-locked, dispersion compensated dye laser using Rhodamine 590 as a gain dye and a $\frac{2}{3}$ mixture of DODCI/DQOCI as a saturable absorber. A one plate Lyot filter was in the cavity. The output train consists of 280 fs pulses at 76 MHz with 0.3 nJ pulse energy tunable from 582 to 593 nm. (This corresponds to an IR range of $1820\text{--}2100\text{ cm}^{-1}$ after mixing with the 527 nm pulses from the regenerative amplifier.) The laser was operated at 591 nm to generate IR at the frequency of the CO stretch (near 2075 cm^{-1}) on Cu(111). The dye laser bandwidth was 100 cm^{-1} . For the frequency domain work, the saturable

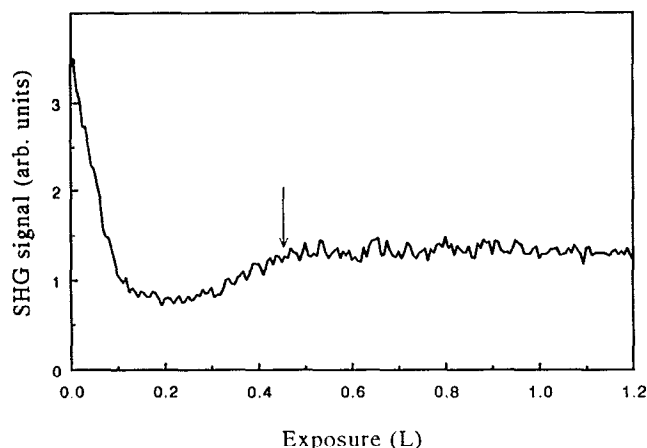


FIG. 2. Variation of surface SHG signal (at 295 nm) from a Cu(111) surface as a function of CO coverage. (1 L = 1×10^{-6} Torr s) The arrow designates the exposure for the $(\sqrt{3} \times \sqrt{3})R30^\circ$ ordered overlayer where the coherent transient measurements were performed.

absorber was removed and a 3 plate Lyot filter was placed in the cavity. The pulses were spectrally narrowed to 2 cm^{-1} and temporally broadened to 10 ps.

The dye pulses were amplified with negligible broadening to 10 μJ in two collinearly pumped dye cells. Short IR pump pulses were generated in an optical parametric amplifier by mixing the amplified dye laser pulse with a portion of a frequency doubled, regeneratively amplified Nd:YLF pulse (400 μJ) in a 1 mm LiIO_3 crystal (type I, 21°). The photon conversion efficiency was $\sim 0.5\%$ and the IR pulse energy was $\sim 5 \text{ nJ}$. For the longer (10 ps) pulses, the IR was generated at 10% conversion efficiency with a 1 cm LiIO_3 crystal resulting in 100 nJ IR pulse energies. After the LiIO_3 crystal the IR and dye pulses were separated and optically delayed. The IR and dye pulses were *p*-polarized with respect to the copper crystal and the beams were recombined and focused on the surface at an incident angle of 72° . The crystal was oriented such that the plane of incidence was along the [211] axis.

Surface SHG from the visible beam provided a convenient monitor of the beam size and CO coverage. The utility of SHG (Refs. 12 and 14) and SFG (Refs. 3, 4, 6, and 15) on surfaces has been demonstrated. The dependence of the SHG signal on CO exposure complemented LEED for monitoring the surface overlayer structure. A typical curve of the SHG signal vs dosage is shown in Fig. 2. As the exposure begins, the signal decreases, reaching a minimum at $\sim 0.2 \text{ L}$, and then increases again. The signal at higher exposures ($> 0.2 \text{ L}$) depends on azimuthal angle. A detailed study of the angular dependence was not pursued here. The dosage curves were reversible upon annealing (i.e., thermal desorption). The SHG signal was sensitive to surface contamination and provided a reproducible method for monitoring the coverages following exposure.

The SHG dosage curves also revealed photodesorption of CO when the dye beam was tightly focused. In particular, photodesorption was indicated by (1) smaller changes in the SHG signal as a function of dosage; (2)

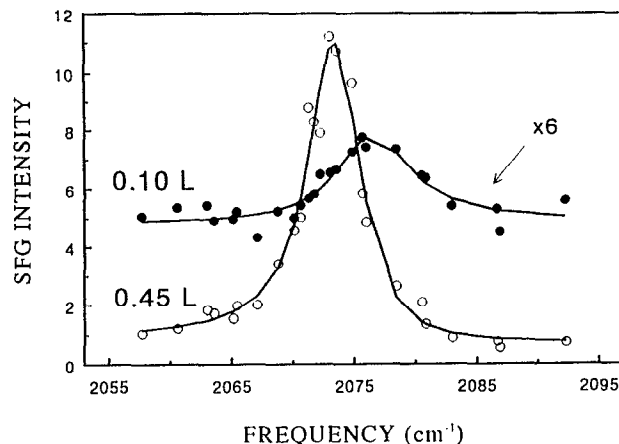


FIG. 3. IR frequency dependence of the surface SFG enhancement for CO on Cu(111) at 93 K for exposures of 0.10 and 0.45 L. The points are the data and the lines are curves derived from the parameters of a least-squares analysis.

further increase of the SHG after dosing had stopped; and (3) irreversible dosing curves upon annealing. While it was possible to focus the lasers to a $250 \mu\text{m}$ diam, the experiments were performed with beam diameters at $500 \mu\text{m}$ to avoid photodesorbing CO from the surface.

The unconverted photons (SFG) were collected outside the chamber and imaged through an interference filter, a 0.5 m double monochromator, and onto a photomultiplier tube (PMT). The SFG signal at 527 nm was measured by gated single photon counting.

For the FID measurements the SFG signal was recorded as a function of the relative IR-visible pulse delay. The peak signal was 6 counts/s with a background of 0.01 counts/s. The frequency domain data were obtained by measuring the SFG signal enhancement as a function of IR laser frequency. The largest signal in this case was about 200 counts/s. These data were acquired by recording the SFG signal for bare copper, and at 0.10 and 0.45 L coverages for a given frequency setting of the IR laser. This procedure minimized systematic errors that are normally introduced by varying the IR frequency at fixed CO coverage.

III. RESULTS

A. Frequency domain experiments

We will first present the frequency domain results. The SFG signal enhancement with respect to bare copper was measured for exposures of 0.10 and 0.45 L of CO on Cu(111) and is shown in Fig. 3. The SFG signal is produced by a nonlinear polarization $P^{(2)}$. $P^{(2)}$ is generated as a result of the nonlinear interaction of input IR [$E(\omega_{\text{ir}})$] and visible [$E(\omega_{\text{vis}})$] electric fields,¹⁶ i.e.,

$$P^{(2)} = \chi^{(2)}(\omega_{\text{sum}} = \omega_{\text{ir}} + \omega_{\text{vis}}) E(\omega_{\text{ir}}) E(\omega_{\text{vis}}), \quad (1)$$

where $\chi^{(2)}$ is the nonlinear second-order susceptibility for the metal-adsorbate system. For CO on Cu(111), we approximate $\chi^{(2)}$ as the sum of two terms,

TABLE I. Parameters derived from a nonlinear least-squares analysis of the surface sum frequency spectra observed for CO on Cu(111). The spectra were fit using the functional form in Eqs. (3) and (4).

	0.10 L	0.45 L
A	0.9	0.9
B	0.9	5.6
2Γ (cm ⁻¹)	6.8(1.6)	4.2(.6)
ω_{10} (cm ⁻¹)	2076.4	2073.6
θ	84(20) ^o	107(30) ^o

$$\chi^{(2)} = \chi_{nr}^{(2)} + \chi_r^{(2)}. \quad (2)$$

Here $\chi_{nr}^{(2)}$ [$\chi_r^{(2)}$] is the nonresonant (resonant) contribution to the susceptibility. The resonant contribution is produced largely by the adsorbates and will be modeled using a standard Lorentzian response function. The nonresonant term contains contributions from the substrate-adsorbate complex. We fit the observed SFG spectra using the following form for the susceptibility:

$$\chi^{(2)} = A e^{-i\theta} - B / (\omega_{10} - \omega_{ir} + i\Gamma_{01}), \quad (3)$$

where A is the magnitude of the frequency independent nonresonant susceptibility, B is the magnitude of the resonant susceptibility, θ is the relative phase between the resonant and "nonresonant" susceptibilities which can arise if the generated is phase shifted by Cu resonances, ω_{01} and ω_{ir} are the vibrational transition center frequency and the laser frequency, respectively, and Γ_{01} is the damping rate for the vibration. In this treatment we assume negligible inhomogeneous broadening. The measured SFG intensity, I_{sfg} is proportional to the square of the nonlinear polarization and therefore to the square of the total susceptibility,

$$I_{sfg} \propto |P|^2 \propto |\chi^{(2)}|^2. \quad (4)$$

SFG spectra display interferences in the form of dispersive line shapes that are caused by cross terms between the resonant and nonresonant susceptibilities (see, for example, Ref. 17). This is seen most clearly in our work for the lower exposure spectrum in which the resonant and nonresonant contributions to the signal are comparable. From an analysis that includes interferences it is possible to determine the relative magnitude and phase of the resonant and nonresonant susceptibilities.

Over the range of IR (and sum) frequencies studied (2055–2095 cm⁻¹), we assumed that the SFG signal from bare copper is constant, and the SFG spectra observed at 0.10 and 0.45 L were fit to the form specified in Eqs. (3) and (4). The line shapes were deconvoluted from the IR laser (assuming a Gaussian with 2 cm⁻¹ intensity bandwidth). Parameters obtained from the analysis are presented in Table I and the best fit line shapes are shown along with the data in Fig. 3. The largest SFG enhancement ($\sim 10\times$) was observed for the higher dosage spectrum at 0.45 L. This curve will generally be a function of incident and azimuthal angles, but we did not study these variations. The peak signal for the spectra did not vary linearly with coverage in part because the lower coverage

band has a broader linewidth thereby reducing the SFG signal. The lower coverage resonance was shifted to higher frequency from 2073.6 to 2076.4 cm⁻¹ and was broadened from 4.2 to 6.8 cm⁻¹. The bandcenters and linewidths determined in this work are consistent with those previously measured using reflection-absorption infrared spectroscopy (RAIRS).¹⁰

This study differs from the FTIR work because we have obtained information about the relative magnitude and phase of the system's *nonresonant* second order susceptibility as a function of coverage. In particular, we observed that the *off-resonance* SFG intensities were within 10% of the bare Cu value, and we found a relatively small variation in the magnitude and phase of the nonresonant susceptibility at coverages of 0.10 and 0.45 L. These observations suggest a simple model for the influence of adsorbed CO on the nonlinear response of the system. Loosely speaking, the nonresonant response of the system can arise from the surface and surface-adsorbate-states at the vacuum-metal interface or from bulk Cu located within one optical skin depth of the metal surface. We have observed that the total nonresonant contribution is relatively insensitive to the presence of the adsorbate. The simplest explanation of this effect is that the nonresonant SFG signal is produced by the bulk Cu at these coverages. Explanations involving the surface layer must either assume that the adsorbate does not appreciably change the polarizability of the surface response or that there are competing effects with different signs. Although unlikely, the latter possibility could, in principle, be investigated further by studying the azimuthal dependence of the signal. Interestingly, the SHG signals depend strongly on adsorbate coverage. This is probably because the UV photons generated in SHG experiments are energetically closer to electronic states of the surface¹⁸ or the surface-adsorbate complex than are the upconverted photons in the SFG measurements.

B. Time domain experiments

We now turn our attention to the time domain experiments. The free induction decay of the vibrational coherence for CO on Cu(111) at a coverage of 0.45 L is shown in Fig. 4. The vibrational coherence is generated using a 380 fs IR pulse. A cross correlation of the IR and visible pulse is also shown in Fig. 4. We found that it was important to incorporate resonant and nonresonant contributions in our analysis to obtain a correct description of the signal variation with time and thereby extract a meaningful dephasing rate.

Our procedure is straightforward. We calculate the total polarization on the surface as a function of time and then compute the upconverted sum frequency field (SFG) as a function of the temporal delay, τ , between the incident visible and infrared fields. Then we square this time-averaged result to get the signal strength. The total polarization is produced by resonant adsorbate molecules *and* nonresonant substrate media.

In this experiment a field $E(t, \tau)$, having both IR and optical frequency components, is used to create a macro-

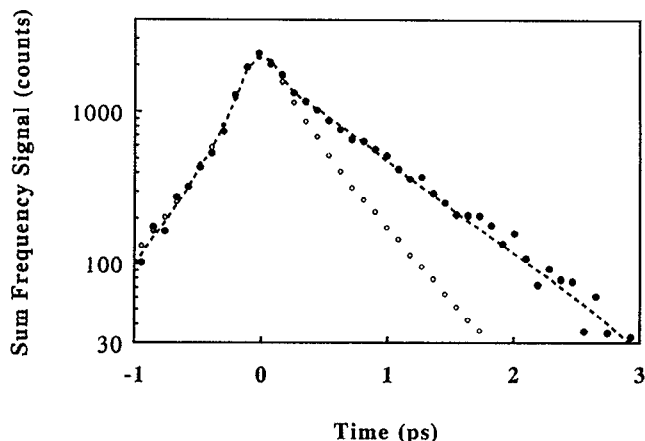


FIG. 4. The variation of the vibrational coherent transient for CO on Cu(111) at 0.45 L measured using 380 fs IR and 280 fs visible pulses as a function of delay. The signal was obtained using surface SFG. The points are the data and the dashed line is the curve obtained using parameters from a least-squares analysis which yields $T_2 = 2 \pm 0.3$ ps. A cross correlation of the visible and IR pulses is shown with open circles.

scopic dipole polarization $P(t, \tau)$ associated with the metal surface and adsorbate. Formally, this polarization arises from the second order response function of the system $R(t_1, t_2)$ and has the canonical form

$$P(t, \tau) = \int_{-\infty}^t dt_1 \int_{-\infty}^{t_1} dt_2 R(t_1, t_2) E(t - t_1, \tau) \times E(t - t_2, \tau). \quad (5)$$

Here we have assumed that the interactions are entirely local. The polarization radiating the signal can be regarded as the dipole moment per unit volume created by the field acting on the surface-adsorbate system through the additional polarizability created by a previous interaction with the field. The IR component of the field, $E_{\text{ir}}(t) \exp(i\omega_{\text{ir}}t)$, is assumed to be centered at $t=0$ while the optical component, $E_v(t - \tau) \exp(i\omega_v t)$, has its envelope peaked at $t - \tau$, where τ is a delay that can be adjusted experimentally. The polarization has oscillatory components at $2\omega_{\text{ir}}$, $2\omega_v$ and $\omega_v \pm \omega_{\text{ir}}$, but the detector is set in the region of $\omega_v + \omega_{\text{ir}}$ so that the detected part of the polarization is

$$P(t, \tau) = \int_{-\infty}^{t_1} dt \int_{-\infty}^{t_1} dt_2 \times \{ R_{\text{iv}}(t_1, t_2) E_{\text{ir}}(t - t_1) E_v(t - t_2 - \tau) \exp[i(\omega_{\text{ir}}t_1 + \omega_v t_2)] + R_{\text{vi}}(t_1, t_2) E_v(t - t_1 - \tau) E_{\text{ir}}(t - t_2) \exp[i(\omega_{\text{ir}}t_2 + \omega_v t_1)] \}, \quad (6)$$

where R_{vi} refers to the response of the surface-adsorbate to the optical field through the polarizability created by the IR field and R_{iv} describes the optically induced polarizability responding to the IR field. The slow response square-law detector cycle averages the field generated at the interface by the material oscillations at $\omega_v + \omega_{\text{ir}}$, thus the signal current for delay τ is proportional to $S(\tau)$, where

$$S(\tau) = \int_{-\infty}^{\infty} dt |P(t, \tau)|^2. \quad (7)$$

Because the optical field has negligible part in driving the linear vibrational response in this experiment and the optical response is fast, the term with R_{iv} at least for τ exceeding the IR pulse duration, interrogates the *free induction decay* of the vibrational coherence. The response R_{vi} decays with the relaxation time of the metal-adsorbate system in the optical frequency regime where there are no known transitions due to the adsorbate. The assumption is made, therefore, that R_{vi} decays much faster than the pulse. The vibrationally resonant part can be simplified assuming the high frequency polarization is very rapidly damped, so that the full sum frequency polarization envelope is given by

$$P(t, \tau) \exp[-i(\omega_{\text{ir}} + \omega_v)t] = E_v(t - \tau) \left\{ i \int_{-\infty}^t dt_1 \alpha E_{\text{ir}}(t_1) \times \exp[(i\Delta + \Gamma_{01})(t_1 - t)] + \beta E_{\text{ir}}(t) \right\}. \quad (8)$$

where β/α is a factor (complex polarizability per unit field) determining the fast response that depends on the magnitude of the metal response at ω_v and ω_{ir} , and determines the ratio of the nonresonant to resonant response of the metal-adsorbate system. This factor is treated as a parameter to be measured by fitting to the data. In a Born-Oppenheimer picture, β is the nonresonant hyperpolarizability [A in Eq. (3)] and α is $\mu' \alpha' \langle q^2 \rangle$, where μ', α' are the CO dipole and polarizability derivatives with respect to displacements q . The detuning from the vibrational resonance is Δ while Γ_{01} is $1/T_2$ for that transition. The form of Eq. (8) makes evident that the induced dipole polarization originates from the optical field $E_v(t - \tau)$ beating with the total linear polarizability which is the part in curly brackets. It follows that $S(\tau)$ has the following form:

$$S(\tau) = \int_{-\infty}^{\infty} dt I_v(t - \tau) |\alpha_{\text{vib}}(t) + \beta E_{\text{ir}}(t)|^2, \quad (9)$$

where $\alpha_{\text{vib}}(t)$ is the complex vibrational polarizability of the CO-surface system, i.e., the first term in curly brackets of Eq. (8). Thus we see that the measured SFG intensity depends in detail on the optical intensity envelope $I_v(t - \tau)$, on the IR *field* envelope, and of course on T_2 . The cross term can significantly modify the interpretation of the data when the duration of the pulses is on the order of T_2 .

One can also describe the upconversion process by starting with the total polarizability $\alpha(t)$ of the adsorbate-substrate system, which can be viewed as a time-dependent quantity produced as a result of a coherent interaction with the input field, $E(t, \tau)$. Then the resultant polarization $P(t, \tau)$ oscillating at $\omega_{\text{ir}} + \omega_v$ is simply $P(t, \tau) = \alpha(t) E(t, \tau)$, and $S(\tau)$ is computed by integrating $|P(t, \tau)|^2$ over all time. The treatments are mathematically equivalent and it is often useful to think of the process in both pictures.

We have fit the data in Fig. 4 using Eq. (9). The temporal profile of the visible pulse intensity was determined from an autocorrelation to be reasonably approximated by a Gaussian with a full width of 280 fs. A cross correlation between the IR and visible pulses (shown in Fig. 4) demonstrated that the full width of the IR pulse was 380 fs. Using these values in the above equation with the field envelopes modeled as Gaussians and with the cross correlation, we determine the total dephasing time to be $T_2 = 2.0 \pm 0.3$ ps. The fit curve from this analysis is shown as the solid line in Fig. 4. If we use sech^2 pulses rather than Gaussian, we find that $T_2 = 1.8 \pm 0.3$ ps. A value of $T_2 = 2.0 \pm 0.1$ ps was also obtained by fitting the decay observed between 2 and 3 ps, i.e., after the driving field is absent, to a single exponential.

The measured dephasing time is related to the full-width at half-maximum $\Delta\nu$ (cm^{-1}), i.e., $\Delta\nu = 1/\pi c T_2$. The measured T_2 corresponds to a linewidth of $\Delta\nu = 5.3 \pm 0.8 \text{ cm}^{-1}$ which is consistent with the value we obtain by our analysis of the frequency domain SFG spectrum as well as with the previous RAIRS measurements (4.5 cm^{-1}).¹⁰

An important result of this study is that the form of the measured FID is fit very well by an *exponential decay* as measured over more than a decade of signal. Thus we predict that the vibrational line shape is homogeneously broadened. A shallow temperature dependence of the linewidth has been measured over the range 95–116 K for the ordered overlayer using FTIR.¹⁰ If the linewidth is assumed to be composed of a temperature *independent* population relaxation (T_1) and temperature dependent pure dephasing, we calculate from their results that the polarization decay is largely due to population relaxation ($T_1 = 1.2$ ps), where the fast relaxation rate is probably due to electron-hole pair coupling. Since the linewidth is very close to being homogeneously broadened, a photon echo would provide essentially the same information on the homogeneous dephasing rate as the free induction decay we have observed for this system. Sufficient inhomogeneous broadening to delay the echo might be present at very low temperature if the relaxation were to lengthen significantly on cooling.

IV. CONCLUSIONS

In summary, we have measured the surface SFG spectrum of CO on Cu(111) at 0.10 and 0.45 L. The analysis accounts for observed interferences that permit a determination of the relative magnitude and phase of the second-order susceptibility. The bandcenter and linewidth parameters are consistent with those found in previous RAIRS studies.

We have also used transient coherent IR spectroscopy to obtain the FID of CO on Cu(111) at 0.45 L. We have analyzed the signal in a manner that incorporates the influence of the pulse envelope to obtain a value of $T_2 = 2 \pm 0.3$ ps. This is the first coherent transient measured for an adsorbate on a metal surface and the fastest transient IR study for a surface adsorbate reported to date. These are the initial results emerging from an ongoing

study of the vibrational dynamics of adsorbates now underway in our laboratory.

Although the present experiment differs from previous ultrafast measurements of adsorbate relaxation on metals,^{2–6} there are important similarities. In each case a very rapid T_1 process depopulates the $v=1$ level and presumably heats the electrons in the metal so that the pure dephasing (T_2') of the CO vibrational transition is slow compared with T_1 at the temperatures employed in the experiments. This measurement of T_1 relaxation can only be accomplished with pulses (T_p) that are shorter than the *total* dephasing time [$T_2 = 2T_1T_2'/(2T_1 + T_2')$]. This means that the experiments must be considered in the coherent limit. This is different from many conventional condensed phase dynamics experiments that fall in the range $T_2 < T_p < T_1$ such that signal decays are naturally governed by the *rate equations* for the populations of the levels. The T_1 relaxation in the coherent limit can be measured by frequency selection of a spontaneous process as shown by Laubereau and Kaiser¹⁹ in the case of vibrations in liquids or by selected pulse sequences such as the stimulated echo.²⁰ The conventional pump-probe method does not provide a clean measurement of T_1 in the coherent limit since the transmitted probe pulse energy depends on both T_1 and T_2 and the material system is expected to oscillate at detuning frequencies. Such effects were observed by Heilweil and co-workers in the transient IR studies of CO on Pt.⁵ Probing the vibrational coherence by sum frequency generation, as pioneered by Harris and Levinos,³ also does not measure T_1 exclusively. Clearly there is a great need for pulse sequence (echo) experiments to probe surface dynamics in the coherent limit. The FID measurements presented here are a first step in this direction.

ACKNOWLEDGMENTS

This work was supported by grants to R. M. H. and A. G. Y. from the NSF through the MRL Program (No. DMR-8519059), to R. M. H. from NSF-CHE and NIH; and to A. G. Y. from the NSF through the PYI Program and the Alfred P. Sloan Foundation.

¹Y. J. Chabal, *Surf. Sci. Rep.* **8**, 211 (1988).

²J. Electron Spectrosc. Relat Phenom. **54/55** (1990); E. J. Heilweil, M. P. Casassa, R. R. Cavanagh, and J. C. Stephenson, *Annu. Rev. Phys. Chem.* **40**, 143 (1989).

³A. L. Harris and N. J. Levinos, *J. Chem. Phys.* **90**, 3878 (1989).

⁴A. L. Harris, L. Rothberg, L. H. Dubois, N. J. Levinos, and L. Dhar, *Phys. Rev. Lett.* **64**, 2086 (1990).

⁵J. D. Beckerle, M. P. Cassassa, R. R. Cavanagh, E. J. Heilweil, and J. C. Stephenson, *Phys. Rev. Lett.* **64**, 2090 (1990); J. D. Beckerle, R. R. Cavanagh, M. P. Cassassa, E. J. Heilweil, and J. C. Stephenson, *J. Chem. Phys.* **95**, 5403 (1991).

⁶S. F. Shane, L. Rothberg, L. H. Dubois, N. J. Levinos, M. Morin, and A. L. Harris, in *Ultrafast Phenomena VII*, edited by C. B. Harris, E. P. Ippen, G. Mourou, and A. H. Zewail (Springer, Berlin, 1990); M. Morin, N. J. Levinos, and A. L. Harris, *J. Chem. Phys.* **96**, 3950 (1992).

⁷P. Guyot-Sionnest, *Phys. Rev. Lett.* **66**, 1489 (1991).

⁸The polarization decay times from the FID measurements in Ref. 7 were 13 and 35 ps at 300 and 120 K, while the pure dephasing time, T_2' , was found to be 85 ps at 120 K.

⁹J. H. Glowia, J. Misewich, and P. P. Sorokin, *Opt. Lett.* **12**, 19 (1987); D. S. Moore and S. C. Schmidt, *ibid.* **12**, 480 (1987); J. M. Jedju and L.

- Rothberg, *Appl. Opt.* **27**, 615 (1988); P. A. Anfinrud, C. Han, and R. M. Hochstrasser, *Proc. Natl. Acad. Sci. USA* **86**, 8387 (1989).
- ¹⁰R. Raval, S. F. Parker, M. E. Pemble, P. Hollins, J. Pritchard, and M. A. Chesters, *Surf. Sci.* **203**, 353 (1988), and references therein.
- ¹¹A. G. Yodh, H. W. K. Tom, G. D. Aumiller, and R. S. Miranda, *J. Opt. Soc. Am. B* **8**, 1663 (1991); A. G. Yodh and H. W. K. Tom, *Phys. Rev. B* **45**, 14302 (1992).
- ¹²J. A. Prybyla, H. W. K. Tom, and G. D. Aumiller, *Phys. Rev. Lett.* **68**, 503 (1992).
- ¹³M. D. Dawson, T. F. Boggess, D. W. Garvey, and A. L. Smirl, *Opt. Commun.* **60**, 791 (1986); M. D. Dawson, D. Maxson, T. F. Boggess, and A. L. Smirl, *Opt. Lett.* **13**, 126 (1988).
- ¹⁴H. W. K. Tom, C. M. Mate, X. D. Zhu, J. E. Crowell, T. F. Heinz, G. A. Somorjai, and Y. R. Shen, *Phys. Rev. Lett.* **52**, 348 (1984); H. W. K. Tom and G. D. Aumiller, *Phys. Rev. B* **33**, 8818 (1986); Y. R. Shen, *Annu. Rev. Phys. Chem.* **40**, 327 (1989); *Nature* **337**, 591 (1989).
- ¹⁵X. D. Zhu, H. Suhr, and Y. R. Shen, *Phys. Rep. B* **35**, 3047 (1987).
- ¹⁶Y. R. Shen, *The Principles of Nonlinear Optics* (Wiley, New York, 1984).
- ¹⁷J. H. Hunt, P. Guyot-Sionnest, and Y. R. Shen, *Chem. Phys. Lett.* **133**, 189 (1987); R. Superfine, P. Guyot-Sionnest, J. H. Hunt, C. T. Kao, and Y. R. Shen, *Surf. Sci.* **200**, 1445 (1988); J. Miragliotta, R. S. Polizotti, P. Rabinowitz, S. D. Cameron, and P. B. Hall, *Chem. Phys.* **143**, 123 (1990); *Appl. Phys. A* **51**, 221 (1990).
- ¹⁸W. Eberhardt and E. W. Plummer, *Phys. Rev. B* **28**, 3605 (1983).
- ¹⁹A. Laubereau and W. Kaiser, *Rev. Mod. Phys.* **50**, 607 (1978).
- ²⁰R. G. Brewer, in *Nonlinear Spectroscopy*, Proceedings of the International School of Physics, Enrico Fermi, Course 64, edited by N. Bloembergen (North Holland, Amsterdam, 1977); T. Mossberg, A. Flusberg, R. Kachru, and S. R. Hartmann, *Phys. Rev. Lett.* **34**, 1523 (1977); R. L. Shoemaker, in *Laser and Coherence Spectroscopy*, edited by J. I. Steinfeld (Plenum, New York, 1978).